Hydraulic Assessment of an Upgraded Pipework Arrangement for the DEMO Divertor Plasma Facing Components Cooling Circuit

P.A. Di Maio[a], R. Burlon[a], G. Mazzone[b], A. Quartararo[a,*], E. Vallone[a], J.H. You[c]

[a]*Department of Engineering, University of Palermo, Viale delle Scienze, Ed. 6, 90128 Palermo, Italy*
[b]*Department of Fusion and Technology for Nuclear Safety and Security, ENEA C. R. Frascati, via E. Fermi 45, 00044 Frascati (Roma), Italy*
[c]*Max Planck Institute of Plasma Physics (E2M), Boltzmann Str.2, 85748 Garching, Germany*

Abstract

In the context of the Work Package DIVertor (WPDIV) of the EUROfusion action, a research campaign has been carried out by University of Palermo in cooperation with ENEA to assess the thermal-hydraulic performances of the DEMO divertor cooling system, concentrating the attention on its 2019 Plasma Facing Components (PFCs) configuration, relevant to DEMO baseline 2017. The research activity has been performed following a theoretical-numerical technique based on the finite volume method (FVM) and adopting the well-known ANSYS CFX CFD code. The PFCs cooling circuit thermal-hydraulic performances under nominal steady-state conditions, assessed mainly in terms of coolant total pressure drop, coolant axial flow speed and margin against Critical Heat Flux (CHF) distributions among the plasma-facing channels, have been evaluated with a CFD analysis to check their compliance with the corresponding limits. Results have highlighted serious critical issues, such as an intolerable total pressure drop (significantly higher than 1.4 MPa) as well as an insufficient margin against CHF onset (lower than 1.4) within all the PFU channels. Therefore, an optimisation study has been performed to investigate the potential improvements of the PFCs cooling circuit thermal-hydraulic performances due to proper changes of its geometric configuration, focussing the attention on the inlet manifold branch. The study has allowed selecting the most effective cooling circuit configuration, that fulfils the maximum pressure drop requirement (Δp <1.4 MPa) while raising the minimum CHF margin within the PFU channels. Moreover, it would allow reducing the ex-vessel total pressure drop, while decreasing the average coolant flow velocity up to values lower than 10 m/s. Models, loads and boundary conditions assumed for the analyses are herewith reported and critically discussed, together with the main results obtained.

Keywords: DEMO, Divertor, Plasma facing components, Thermofluid-dynamics, CFD analysis

1. Introduction

The European research roadmap, drafted to realize commercially viable fusion power generation, has defined reliable power exhausting as one of the most critical missions. Heat-exhaust systems must be capable of withstanding the large heat and particle fluxes of a fusion power plant, allowing, at the same time, as high performance as possible from the core plasma [1].

The divertor is the key in-vessel component in this context. Being responsible for power exhaust and impurity removal via guided plasma exhaust, the viability of fusion power generation heavily depends indeed on the heat load that can be tolerated by the divertor under normal and off-normal operation [2]. Therefore, particular attention has to be paid to the thermal-hydraulic design of its cooling system, to ensure a uniform and proper cooling, without an unduly high pressure drop.

In the context of the Work Package DIVertor (WPDIV) [3, 4] of the EUROfusion action and in line with previous research activities [5, 6, 7, 8, 9], a research campaign has been carried out by University of Palermo (UNIPA) in cooperation with ENEA to assess the thermal-hydraulic performances of the DEMO divertor Plasma Facing Components (PFCs) cooling circuit.

Attention has been initially focussed on the layout of the PFCs cooling circuit released in early 2019 and consistent to DEMO Baseline 2017 [10], assessing its steady-state thermal-hydraulic performances. These lat-

*Corresponding author
Email address: andrea.quartararo@unipa.it (A. Quartararo)

ter shall comply with the requirements on pressure drop (Δp < 1.4 MPa) and CHF margin (>1.4) [11], while providing a uniform flow distribution among PFU channels.

Then, according to the issues arisen from this first thermal-hydraulic assessment, the PFCs cooling circuit layout has been optimised focussing the attention on the inlet manifold branch, thus allowing for a significant pressure drop reduction.

As a consequence, a second optimised PFCs cooling circuit layout has been released in 2019, taking into account both the indications given by thermal-hydraulic calculations and some manufacturing considerations [12]. The thermal-hydraulic performances of this upgraded PFCs cooling circuit have been numerically assessed under nominal steady-state conditions to check if the aforementioned requirements are met.

The research activity has been performed following a numerical technique based on the Finite Volume Method (FVM) and adopting the well-known ANSYS CFX v.19.2 R1 Computational Fluid-Dynamic (CFD) code [13]. The same approach has been already used by authors in similar studies [14] and adopted to evaluate concentrated hydraulic resistances to be used in system codes [15, 16]. Models, assumptions and boundary conditions are reported in the following and thoroughly discussed, alongside the main results obtained.

2. The 2019 DEMO divertor and PFCs cooling system

In conformity with its 2019 design [11], the DEMO divertor consists of 48 toroidal assemblies (divertor cassettes). Each one includes a Cassette Body (CB), endowed with a Liner and two Reflector Plates (RPs), that supports two PFCs (fig. 1). These latter are named Inner and Outer Vertical Target (IVT, OVT), and are comprised of actively cooled Plasma Facing Units (PFUs) equipped with Swirl Tape (ST) turbulence promoters.

The cooling scheme adopted for the DEMO divertor, developed by the cooperation between UNIPA thermal-hydraulic research unit and the Divertor CAD team, consists of two circuits designed to independently cool the Eurofer components (CB, Liner and RPs) and the PFCs. The focus of this paper is the PFCs cooling circuit (fig. 2), characterised by two main sections, devoted to separately cool the 31 plasma-facing channels of the IVT and the 43 channels of the OVT, connected in parallel by three-way branching to the inlet and outlet manifolds.

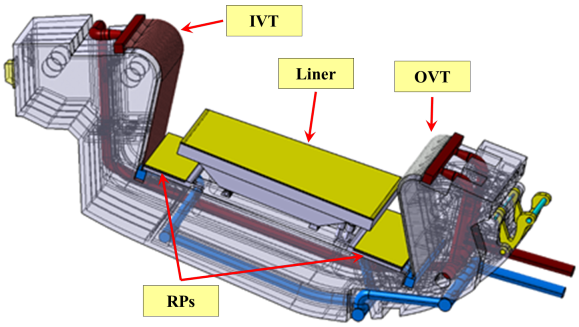

Figure 1: DEMO Divertor cassette (Design 2019).

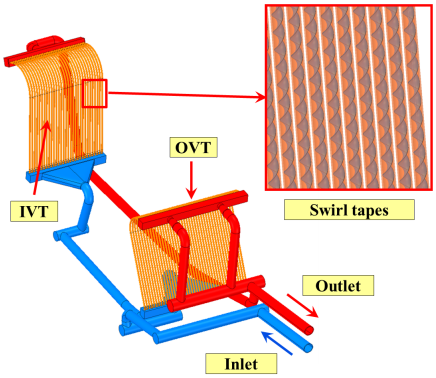

Figure 2: DEMO Divertor PFCs (Design 2019).

3. PFCs cooling circuit CFD analysis

The thermal-hydraulic performances of the PFCs cooling circuit under the coolant operating conditions of table 1 [11] have been assessed by running steady-state, isothermal CFD analyses, where the temperature of the fluid inside the PFCs has been supposed to be equal to the average value between inlet and outlet sections, evaluated by means of simple thermodynamic calculations. Moreover, realistic configurations with swirl tape turbulence promoters inside each PFU cooling channel have been considered.

Table 1: Summary of PFCs coolant operating conditions.

	Reference Conditions
Inlet Pressure [MPa]	5.0
Inlet Temperature [°C]	130
Removed Power [MW]	136
G per Cassette [kg/s]	98.63

The mesh parameters selected for the PFCs cooling circuit are reported in table 2, while some details of the mesh set up for the CFD analysis are shown in fig. 3.

Furthermore, the adopted main assumptions, models and Boundary Conditions (BC) are reported in table 3. It is worth to underline that the considered meshing methodology and numerical technique have been chosen following the outcomes of previous validation and mesh sensitivity analyses. In particular, they have been selected in order to guarantee a good compromise between solution accuracy and computational costs.

Table 2: Summary of the main mesh parameters.

Mesh Parameter	Value
Nodes	$4.0{\cdot}10^{7}$
Elements	$5.5{\cdot}10^{7}$
Elements Topology	Hybrid (Tetras/Wedges)
Inflation Layers Number	12
First Layer Thickness [μm]	12
Layers Growth Rate	1.4
Typical Element Size [m]	$2.39{\cdot}10^{-3}$
Surface with y^+ <100 [%]	100

Table 3: Summary of PFCs CFD analysis setup.

	Reference Conditions
Analysis Type	Steady-state Isothermal
Material Library	Water IAPWS IF97 [17]
Temperature [°C]	133
Turbulence Model	k-ϵ
Boundary Layer Modelling	Scalable Wall Functions
Absolute Wall Roughness [μm]	2
Inlet Pressure [MPa]	5
Outlet Mass Flow Rate [kg/s]	98.63

The coolant total pressure contour is shown in fig. 4, while total pressure drops across the main sections of the PFCs cooling circuit (fig. 5) are reported in table 4. In particular, it is worth noticing that the presence of the ST turbulence promoters is clearly shown by IVT and OVT high pressure drops.

Table 4: PFCs cooling circuit total pressure drop distribution.

Sections	Pressure points	Δp [MPa]
Inlet Manifold	**IM_A - IM_B**	0.4455
IVT Inlet 3Way	**IM_B - IVT_A**	0.7543
Inlet IVT Manifold	**IVT_A - IVT_B**	0.0688
IVT	**IVT_B - IVT_C**	0.7429
Outlet IVT Manifold	**IVT_C - IVT_D**	0.0581
IVT Outlet 3Way	**IVT_D - OM_A**	0.1781
OVT Inlet 3Way	**IM_B - OVT_A**	0.6887
OVT	**OVT_A - OVT_B**	0.9180
OVT Outlet 3Way	**OVT_B - OM_B**	0.2658
TOTAL	**IM_A - OM_B**	**2.3179**

As it may be argued from the obtained results, the

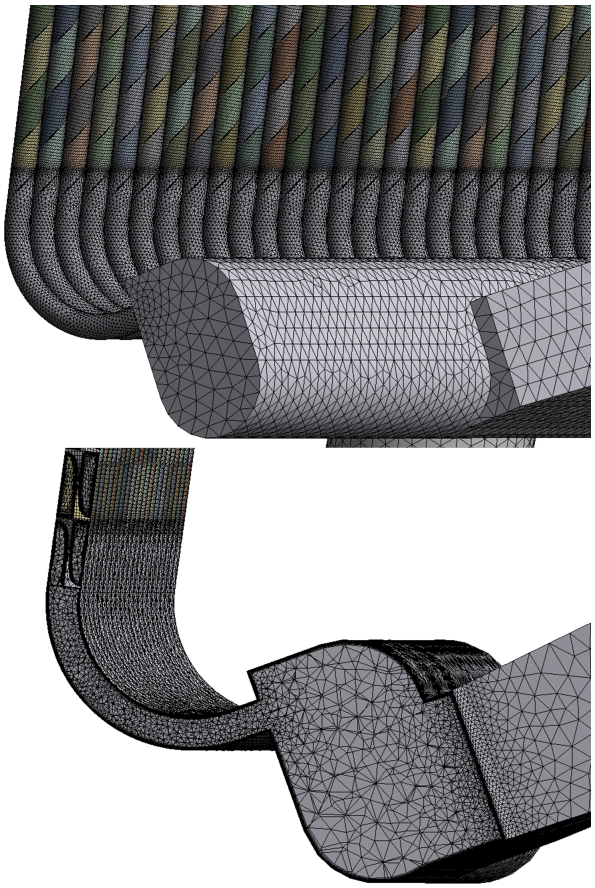

Figure 3: Mesh adopted for PFCs cooling circuit CFD analysis.

PFCs cooling circuit overall total pressure drop amounts to ≈2.3 MPa, resulting significantly higher than the prescribed limit of 1.4 MPa. It is worth highlighting that most of the overall total pressure drop (≈0.9 MPa) is located at the 3-way connections between inlet/outlet manifolds and OVT/IVT branching with particular reference to the inlet connection (≈0.7 MPa), as reported in table 4, posing then the need for a deep revision of the cooling circuit pipework.

Additionally, in order to check whether unbalanced distributions might take place within the circuit preventing a uniform cooling of its solid components, the distributions of the coolant axial flow velocity among the PFU channels of both the VTs have been assessed and they have been reported in fig. 6, summarising their key-parameters in table 5.

From the analysis of the results obtained, it may be argued that the distribution of coolant axial flow velocity is acceptably uniform for each PFU channel, for both the VTs, since maximum deviations in the order of

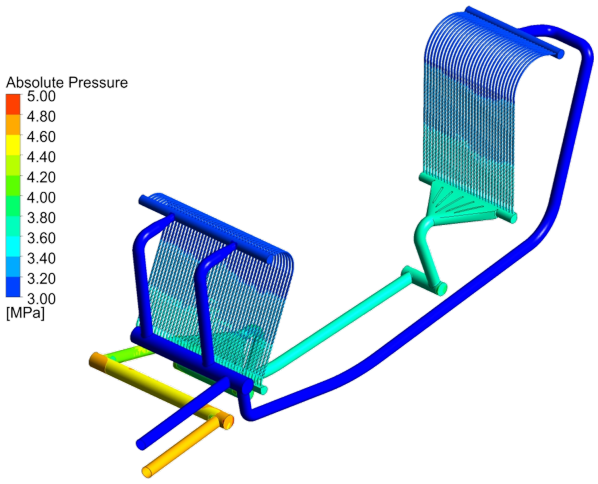

Figure 4: PFCs coolant total pressure field.

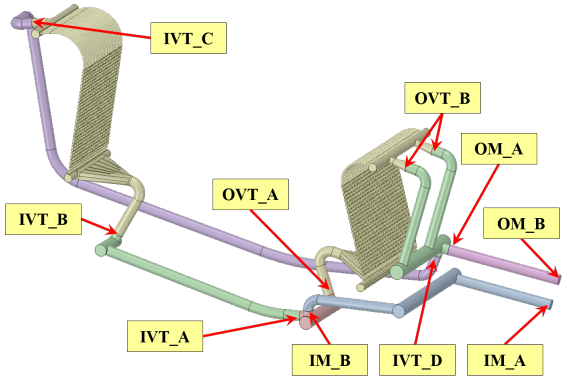

Figure 5: PFCs cooling circuit main sections.

8% and 7% have been estimated between the maximum (Max V_{ax}) and minimum (Min V_{ax}) values calculated as for OVT and IVT, respectively. As a further confirmation, the standard deviations calculated for both the two axial flow velocity distributions amount to ≈0.3 and ≈0.2 m/s, respectively, resulting to be quite low.

It is important to remark that the coolant temperature rise within the PFCs is so modest (≈6°C) that the local variations of water properties would not be able to significantly affect the coolant velocity distribution among PFU channels and between VTs. As a consequence, the assumption of isothermal flow can be undoubtely considered well-founded.

The distributions of the CHF margin within plasma-facing channels of both the VTs have been assessed so to make sure that its prescribed minimum value of 1.4 is ensured by the present layout. Attention has been devoted to the strike point sections of VTs, where the

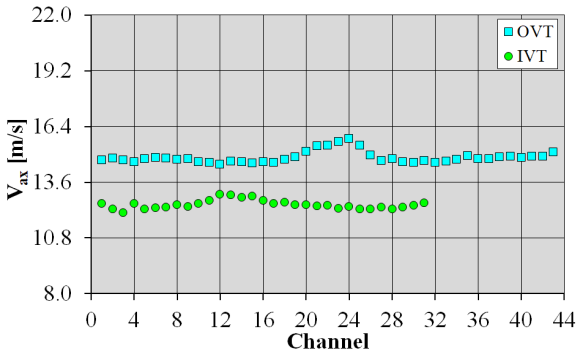

Figure 6: Coolant axial flow velocity distribution among OVT and IVT PFU channels.

Table 5: Coolant axial flow velocity distribution key-parameters.

	OVT	**IVT**
Max V_{ax} [m/s]	15.78	12.98
Min V_{ax} [m/s]	14.51	12.06
$\epsilon_{Max-Min}$**[%]**	8.03	7.14
Average V_{ax} [m/s]	14.83	12.47
Std. Deviation [m/s]	0.31	0.22

peak heat flux (20 MW/m^2 [11]) is supposed to be positioned. Adopting the methodology described in [7], which is based on the correlation of [18], the CHF at the channel walls has been evaluated for each PFU channel. The obtained distributions have been reported in fig. 7 alongside their key-parameters in table 6. From the

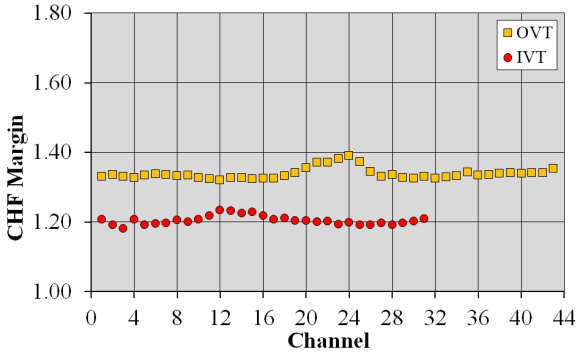

Figure 7: CHF margin distribution among OVT and IVT PFU channels.

analysis of the results obtained, it may be argued that, despite the calculated distributions of CHF margin are acceptably uniform for both the VTs, the CHF margin values calculated for both VTs PFU channels result always lower than the prescribed limit of 1.4.

Table 6: Coolant axial flow velocity distribution key-parameters.

	OVT	IVT
Max CHF Margin	1.34	1.35
Min CHF Margin	1.24	1.27
$\epsilon_{Max-Min}$**[%]**	7.16	5.60
Average CHF Margin	1.27	1.29
Std. Deviation	0.03	0.01

4. Design optimization

The performed analyses have highlighted the need for a revision of the PFCs layout, mainly intended to reduce both distributed and concentrated hydraulic resistances at the inlet/outlet manifold branches. Therefore, focussing the attention on the inlet manifold branch of the analysed PFCs layout, the thermal-hydraulic behaviour of selected revised configurations has been assessed by running local, steady-state, isothermal CFD analyses.

At first, since both distributed and concentrated hydraulic resistances strongly depends on the manifold hydraulic diameter, it has been decided to investigate the potential effect of the manifolds diameter increase on the total pressure drop reduction. Therefore, it has been considered a revised inlet manifold branch layout, namely V0.1, characterized by inlet common manifold diameter increased from 70 mm to 98 mm and single PFC manifold diameter increased from 70 mm to 75 mm. A comparison between the original inlet manifold branch configuration and the configuration V0.1 is shown in fig. 8. Results show that the total pressure

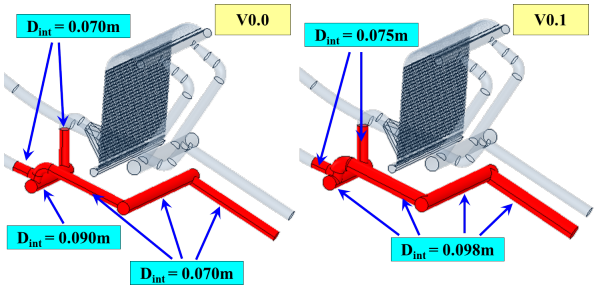

Figure 8: PFCs inlet branching V0.0 and V0.1 layout comparison.

drop calculated for the original inlet manifold branch configuration amounts to 1.248 MPa, in agreement with the results obtained for the complete PFCs cooling circuit. Conversely, the total pressure drop predicted for the configuration V0.1 amounts to 0.935 MPa with a margin from the original layout of 0.313 MPa (≈25%).

As a second step, in order to further reduce the contribution of the inlet manifold branch to the overall total pressure drop, it has been conceived a revised inlet manifold branch layout, namely V1.1, where sharp elbows have been replaced by smooth curves and the branch layout has been modified so to ease coolant flowing towards the PFCs while keeping unaltered the pipe scheme and the manifold diameters. Configuration V1.1 is shown in fig. 9 along with the original one. Results

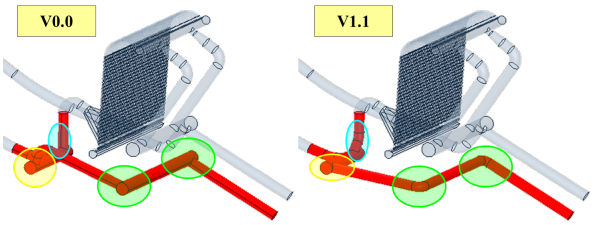

Figure 9: PFCs inlet branching V0.0 and V1.1 layout comparison.

show that the total pressure drop calculated for the configuration V1.1 amounts to 0.307 MPa with a margin from the original layout of 0.941 MPa (≈75%). The considered solution might fulfil the maximum pressure drop requirement (Δp < 1.4 Mpa). Nevertheless, total pressure drop along the PFCs cooling circuit shall be further reduced, whenever possible, in order to increase as much as possible the average total pressure and thus the minimum CHF margin within the PFU channels. Moreover, layout simplification might help manufacturing and remote maintenance procedures.

Therefore, a third revised inlet manifold branch layout, namely V2.0, has been conceived. A comparison between the configuration V1.1 and configuration V2.0 is shown in fig. 10. Results show that configuration

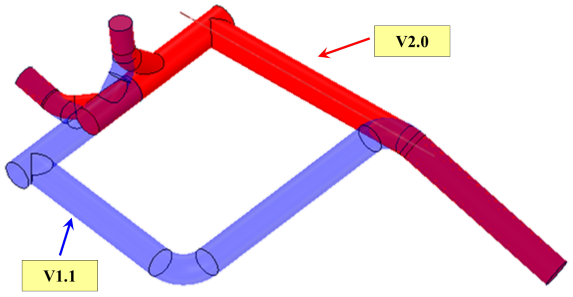

Figure 10: PFCs inlet branching V1.1 and V2.0 layout comparison.

V2.0 has allowed a further pressure drop reduction of 0.113 MPa with an overall margin from the original layout of 1.055 MPa (≈85%).

At a later stage, a further design change has been deemed necessary following some considerations of the

Work Package Balance of Plant (WPBoP). In fact, considering the present PFCs cooling circuit layout (V0.0), an average coolant flow velocity of ≈28 m/s may be calculated for the feeding manifolds that brings to an average pressure drop per unit length of ≈0.1 MPa/m and, consequently, to an unacceptably high pumping power. Therefore, it has been issued a revised inlet manifold branch layout, namely V2.1, that is characterized by DN125 and DN90 (sch. 10) pipes for the common manifolds and for the OVT/IVT manifolds, respectively, aiming at reducing the ex-vessel total pressure drop while decreasing the average coolant flow velocity up to values lower than 12 m/s [19]. A visual comparison of configurations V2.0 and V2.1 is shown in fig. 11. Results show that configuration V2.1 has al-

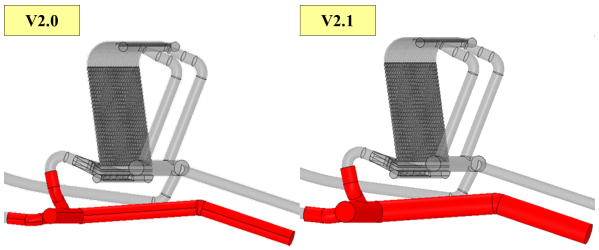

Figure 11: PFCs inlet branching V2.0 and V2.1 layout comparison.

lowed a further pressure drop reduction of 0.139 MPa with an overall margin from the original layout of 1.194 MPa (≈96%). As an additional improvement, configuration V2.1 has allowed to reduce the ex-vessel total pressure drop per unit length up to ≈0.004 MPa/m, which is totally in line with the needs of the WPBoP, while decreasing the average coolant flow velocity up to a value of ≈8 m/s.

The results of the selected inlet manifold branch optimization loop are summarized in table 7 and in fig. 12.

Table 7: PFCs cooling circuit inlet branching optimization summary.

Version	Δp [MPa]	Δ(Δp) [MPa]
V0.0	1.2481	-
V0.1	0.5465	0.7016
V1.1	0.3068	0.9413
V2.0	0.1934	1.0547
V2.1	0.0545	1.1936

5. Upgraded PFCs cooling circuit CFD analysis

On the basis of the optimization results and of some manufacturing considerations, the Divertor CAD team revised the PFCs cooling circuit layout, introducing similar improvements also for the outlet manifold

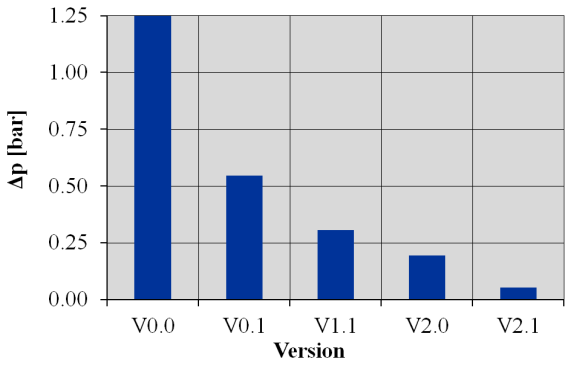

Figure 12: PFCs cooling circuit inlet branching optimization summary.

branching schemes. The mesh parameters selected for the considered PFCs cooling circuit are similar to those reported in table 2, while the adopted main assumptions, models and boundary conditions are the same of table 3.

The coolant pressure spatial distribution for the upgraded configuration is reported in fig. 13, while total pressure drops contributions are reported in table 8 for the main sections of the circuit (fig. 5). As it may be ar-

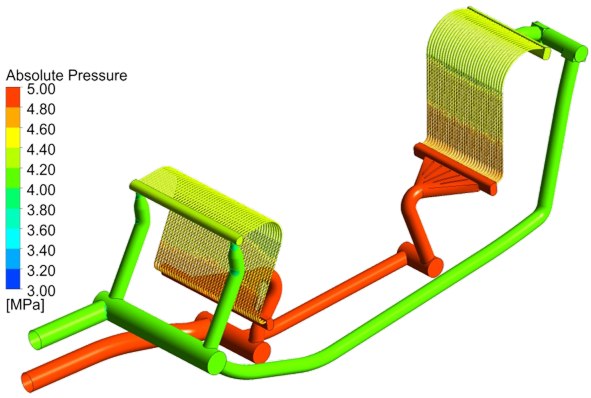

Figure 13: PFCs coolant total pressure field.

gued from the obtained results, the upgraded PFCs cooling circuit overall total pressure drop is equal to ≈0.94 MPa, resulting considerably lower than 1.4 MPa, compliant wih the prescribed limits. In particular, the optimised PFCs cooling circuit shows its effectiveness at the OVT/IVT branches, where the total pressure drop was reduced by more than 90% with respect to the baseline PFCs design.

In addition, the distributions of the coolant axial flow velocity among the PFU channels of both the VTs have

Table 8: PFCs cooling circuit total pressure drop distribution.

Sections	Pressure points	Δp [MPa]
Inlet Common Manifold	**IM_A - IM_B**	0.0038
IVT Inlet 3Way	**IM_B - IVT_A**	0.0541
Inlet IVT Manifold	**IVT_A - IVT_B**	0.0311
IVT	**IVT_B - IVT_C**	0.7958
Outlet IVT Manifold	**IVT_C - IVT_D**	0.0229
IVT Outlet 3Way	**IVT_D - OM_A**	0.0358
OVT Inlet 3Way	**IM_B - OVT_A**	0.0581
OVT	**OVT_A - OVT_B**	0.8815
OVT Outlet 3Way	**OVT_B - OM_B**	0.0002
TOTAL	**IM_A - OM_B**	**0.9436**

been reported in fig. 14 along with their key-parameters in table 9.

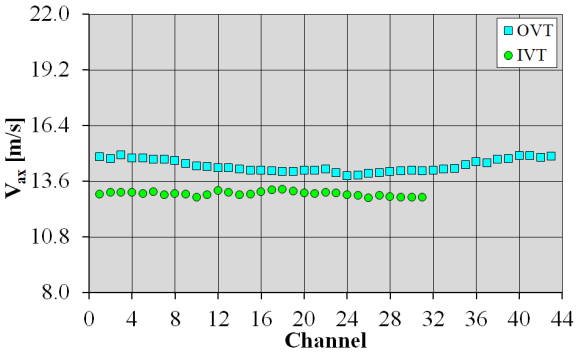

Figure 14: Coolant axial flow velocity distribution among OVT and IVT PFU channels.

Table 9: Coolant axial flow velocity distribution key-parameters.

	OVT	IVT
Max V_{ax} [m/s]	14.91	13.18
Min V_{ax} [m/s]	13.85	12.76
$\epsilon_{Max-Min}$**[%]**	7.11	3.18
Average V_{ax} [m/s]	14.37	12.95
Std. Deviation [m/s]	0.32	0.12

From the analysis of the results obtained, it may be argued that the distribution of coolant axial flow velocity within PFU channels is acceptably uniform for both the VTs, with values in line with the baseline configuration.

Concerning the distributions of the margin against CHF onset within the VTs PFU cooling channels, they have been reported in fig. 15 along with their main parameters in table 10.

From the analysis of the results obtained, it may be argued that the calculated distributions of CHF margin are acceptably uniform both for both the IVT and OVT,

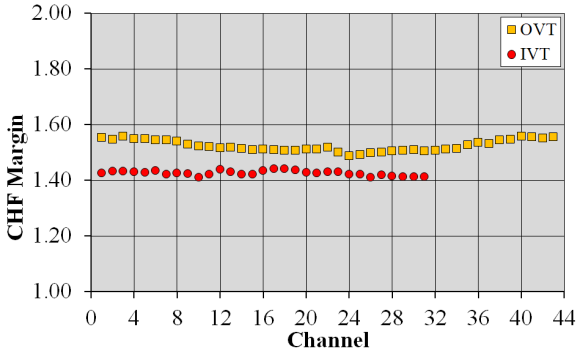

Figure 15: CHF margin distribution among OVT and IVT PFU channels.

Table 10: Coolant axial flow velocity distribution key-parameters.

	OVT	IVT
Max CHF Margin	1.56	1.44
Min CHF Margin	1.49	1.41
$\epsilon_{Max-Min}$**[%]**	4.51	2.15
Average CHF Margin	1.52	1.43
Std. Deviation	0.02	0.01

since deviations between their pertaining maximum and minimum values amount to less than 5%. Moreover, the values of CHF margin calculated for both VTs PFU channels result higher than the limit of 1.4 in every single PFU channels, being its lowest value equal to 1.41. It is worth mentioning how the CHF margin improvement with respect to the baseline PFCs cooling circuit design can be related to the reduced pressure losses inside the circuit.
As a matter of fact, an increment of the average pressure inside the circuit increases the CHF value, thus improving the CHF margin.

6. Conclusions

Within the framework of the activities promoted by the EUROfusion consortium, University of Palermo in cooperation with ENEA carried out a research campaign to evaluate the thermal-hydraulic performances of DEMO divertor cassette cooling system, posing the attention on the PFCs cooling circuit 2019 configuration. A theoretical-numerical approach based on the FVM has been followed adopting the well-known ANSYS CFX CFD code.

The PFCs cooling circuit nominal thermal-hydraulic behaviour has been assessed to evaluate coolant total pressure drop, flow velocity and CHF margin distributions within the PFU channels. Obtained results in-

dicated a pressure drop significantly higher than the agreed limit and amounting to ≈2.32 MPa, mainly due to the hydraulic resistances of the 3-way connections between inlet/outlet manifolds and OVT/IVT branching. Therefore, in order to evaluate the potential thermal-hydraulic performance improvement related to a design revision of these components, a localized optimization study has been performed, showing a good margin to reduce the overall pressure drop.

Based of the optimization results, a revised PFCs cooling circuit layout has been devised that allowed to obtain a significantly lower pressure drop, amounting to ≈0.94 MPa, and an improvement of both flow uniformity and CHF margin inside the PFU channels.

CRediT authorship contribution statement

P.A. Di Maio: Conceptualization, Methodology, Investigation, Writing - original draft. **R. Burlon**: Conceptualization, Methodology, Investigation, Writing - original draft. **G. Mazzone**: Conceptualization, Methodology, Investigation, Writing - original draft. **A. Quartararo**: Conceptualization, Methodology, Investigation, Writing - original draft. **E. Vallone**: Conceptualization, Methodology, Investigation, Writing - original draft. **J.H. You**: Conceptualization, Methodology, Investigation, Writing - original draft.

Declaration of Competing Interest

The authors declare that they have no known competing financial interests or personal relationships that could have appeared to influence the work reported in this paper.

Acknowledgments

This work has been carried out within the framework of the EUROfusion Consortium and has received funding from the Euratom research and training programme 2014-2018 and 2019-2020 under grant agreement No 633053. The views and opinions expressed herein do not necessarily reflect those of the European Commission.

References

[1] T. Donné, W. Morris, European Research Roadmap to the Realisation of Fusion Energy, 2018, ISBN: 978-3-00-061152-0.

[2] G. Federici, et al., Overview of the DEMO staged design approach in Europe, Nuclear Fusion 59 (2019) 066013. doi:10.1088/1741-4326/ab1178.

[3] J.H.You, et al., Conceptual design studies for the European DEMO divertor: Rationale and first results, Fusion Engineering and Design 109–111 (2016) 1598–1603. doi:10.1016/j.fusengdes.2015.11.012.

[4] J.H.You, et al., Progress in the initial design activities for the European DEMO divertor: Subproject "Cassette", Fusion Engineering and Design 124 (2017) 364–370. doi:10.1016/j.fusengdes.2017.03.018.

[5] P.A. Di Maio, et al., Thermal-hydraulic behaviour of the DEMO divertor plasma facing components cooling circuit, Fusion Engineering and Design 124 (2017) 415–419. doi:10.1016/j.fusengdes.2017.02.025.

[6] P.A. Di Maio, et al., On the thermal-hydraulic optimization of DEMO divertor plasma facing components cooling circuit, Fusion Engineering and Design 136 (2018) 1438–1443. doi:10.1016/j.fusengdes.2018.05.032.

[7] P.A. Di Maio, et al., Hydraulic analysis of EU-DEMO divertor plasma facing components cooling circuit under nominal operating scenarios, Fusion Engineering and Design 146 (2019) 1764–1768. doi:10.1016/j.fusengdes.2019.03.030.

[8] G. Mazzone, et al., Structural verification and manufacturing procedures of the cooling system, for DEMO divertor target (OVT), Fusion Engineering and Design 146 (2019) 111919. doi:10.1016/j.fusengdes.2019.02.139.

[9] P.A. Di Maio, et al., On the numerical assessment of the thermal-hydraulic operating map of the DEMO Divertor Plasma Facing Components cooling circuit, Fusion Engineering and Design 161 (2020). doi:10.1016/j.fusengdes.2020.111919.

[10] C. Gliss, DEMO Baseline Model 2017, 2017, EUROfusion IDM Ref.: 2N4EZW.

[11] G. Mazzone, et al., Eurofusion-DEMO Divertor - Cassette Design and Integration, Fusion Engineering and Design 157 (2020) 111656. doi:10.1016/j.fusengdes.2020.111656.

[12] U. Bonavolontà, et al., EU-DEMO divertor: Cassette design and PFCs integration at pre-conceptual stage, Fusion Engineering and Design 159 (2020). doi:10.1016/j.fusengdes.2020.111784.

[13] ANSYS Inc., ANSYS CFX-Solver Theory Guide, 2019, Release: 2019 R1.

[14] P.A. Di Maio, et al., On the hydraulic behaviour of ITER Shield Blocks #14 and #08. Computational analysis and comparison with experimental tests, Fusion Engineering and Design 109-111 (2016) 30–36. doi:10.1016/j.fusengdes.2016.03.060.

[15] P.A. Di Maio, et al., Analysis of the steady state hydraulic behaviour of the ITER blanket cooling system, Fusion Engineering and Design 98-99 (2015) 1470–1473. doi:10.1016/j.fusengdes.2015.05.070.

[16] P.A. Di Maio, et al., Numerical simulation of the transient thermal-hydraulic behaviour of the ITER blanket cooling system under the draining operational procedure, Fusion Engineering and Design 98-99 (2015) 1664–1667. doi:10.1016/j.fusengdes.2015.01.024.

[17] International Association for the Properties of Water and Steam, Revised Release on the IAPWS Industrial Formulation 1997 for the Thermodynamic Properties of Water and Steam, 2007.

[18] A.R. Raffray, et al., Critical heat flux analysis and R&D for the design of the ITER divertor, Fusion Engineering and Design 45 (4) (1999) 377–407. doi:10.1016/S0920-3796(99)00053-8.

[19] A. Natalizio, J. Collén, Final Report on SEAFP Task M8 COOLING SYSTEM DESIGN PART A: WATER COOLANT OPTION, 1994, SEAFP/R-M8/F(94).